

Design Theory of Equal Split Dual- Band Power Divider without Reactive Elements

Natarajamani S, and Rekha G Nair

Department of Electronics and Communication Engineering, Amrita School of Engineering, Coimbatore, Amrita Vishwa Vidyapeetham, India.

Corresponding author: Natarajamani S (e-mail: s_natarajamani@cb.amrita.edu)

ABSTRACT This paper presents a design approach for getting dual-band working in a Wilkinson-based power divider (WPD) without adding any reactive elements or open- or short-circuited stubs. The transfer matrix approach is used to get the analytical solutions of the required design equations. Admittance representation with respect to the input and output ports is done to perform an even-odd mode analysis. Each section's impedance is kept constant, but the electrical length varies. Different combinations of electrical lengths are taken such that the overall length remains constant. The electrical lengths are selected based on dual-band analysis and depend on the tuning ratio. The conditions for attaining the impedance matching are applied to the obtained design equations and hence found the values of the matching resistors to be placed between the transmission line sections. The proposed power divider centered at 2.5GHz and 7GHz is theoretically calculated, simulated, and fabricated. Finally, design procedures and experiments show good agreement with theoretical simulation.

INDEX TERMS Dual-band, matching resistors, reactive elements, transmission line, Wilkinson Power Divider.

I. INTRODUCTION

IN microwave and wireless communication systems power dividers are inevitable devices. They usually find applications in devices like mixers, array antennas, modulators, and demodulators. They can divide the input signal into multiple output signals or mix two signals [1]. WPD is the practically and popularly most widely used type of power divider. Even-Odd Mode analysis method provides easy analysis of WPDs with equal power division [2].

Structures for multi-band operation based on different approaches are also proposed in the literature. A coupled-line circuit for a dual-band WPD with two coupled lines with different characteristic impedances and two lumped resistors is presented in [3].

A wide variety of PD's with multiple operating bands exists. Dual-band (DB) WPDs having two-section transmission lines and resistors are proposed in [3]. This design has a high range of designable frequencies, and by replacing transmission line sections with dual-band transformers, the spurious bands emerging between the two passbands are eliminated. Using this method of dual-band transformers, an additional band of isolation is also obtained at the centre frequency. By adding reactive elements like parallel LC circuits or series LC circuits for isolation, the DB operation will give the needed range of frequency ratio [4, 5]. A Wilkinson-type power divider using lumped elements to attain unequal division of

power and two operating bands is proposed here.

Two-segment transformers with parallel LC circuits on centre points are the adopted technique. Edge-open Split Ring Resonator type dual-band bandpass filter is proposed in [6]. Dual-band bandpass Wilkinson power divider (WPD) implemented with quarter-wavelength stepped-impedance resonators and inverters is presented in [7]. The passband is controlled with the DB resonators and inverters. A DB PD based on a segmented transmission line is presented in [8]. A Power divider with two arbitrary working frequencies and load impedance in a wide range was proposed in [9]. A complex network for port isolation and improvement in bandwidth is presented in [10]. The circuit also provides improved isolation bandwidth. So the use of artificial transmission lines, coupled lines, the addition of stubs, stepped impedance transformers, and a combination of parallel and series RLC circuits are some of the different techniques adopted in literature to provide dual-band operation. The periodic loading of conventional TL with capacitors to get port extended DB PD is presented in [11].

A microstrip antenna on cement substrate suitable for WLAN, Fibre to the Home Etc. is presented in [12]. A dual-band divider with independent power division ratios is presented in [13] dual-band; a grounded resistor, phase inverter, and four transmission-line sections are used in this design. Compact dual-band WPD having frequency-dependent com-

plex impedance termination is proposed in [14]. The coupled lines, Provide FDCI matching. A microstrip patch antenna based on dimension adjustment of the fractal defected ground structure for enhancing the bandwidth is presented in [15]. Dual-band WPD without transmission line stubs additional lumped elements is presented in [16]. L-type transmission lines are used here. In comparison with conventional PDs, only three additional TLs are employed.

Dual-band WPD where frequency bands are obtained by using series stub to replace the quarter-wavelength transmission is designed in [17] lines in the conventional design by two compact ones separated by a series stub. A DB Wilkinson power divider is implemented based on an integrated passive device process with a common inductor, and two shunt inductors are presented in [18].

The parasitic effects occur due to the presence of lumped reactance elements as frequency increases, chip capacitance, and inductance vary and hence deviate from the upper-frequency band and restrict the wideband performance, so reactive elements are unsuitable for applications at high frequency. Asymmetric characteristic impedance with open and closed stub configuration and single isolation resistor is used here; hence a distributed structure without reactive elements and unequal power division is presented. PD's lack of reactive elements is a new challenge in multi-band power divider research. The design theory of a WPD working in two arbitrary bands is presented in this paper. Several approaches in this regard are there. However, in this paper, the novelty is that the impedance of transmission line sections is kept constant, and the physical length is changed based on different combinations of electrical lengths. The total electrical length is unchanged. Even though two different physical lengths of TLs are used, matching resistors placed between the cascaded sections help achieve multi-band operation.

The organization of the paper is as follows. Section II explains the design theory and analytical equations needed in the structure's design. The implementation and measurements obtained are analyzed in section III, and the work concludes in section IV.

II. ANALYTICAL SOLUTION AND DESIGN THEORY FOR THE PROPOSED POWER DIVIDER WITH DUAL BANDS

The model of the dual-band equal split power divider is given in Fig. 1. This structure has two sections of transmission lines. The two sections are cascaded by matching resistors. The impedance of cascaded transmission line sections are taken as $Z_{TL1} = Z_{TL2} = Z_{TL}$ and the total electrical length of the structure is taken as $\theta = 180^\circ$.

The first transmission line section in the cascade is provided with a matching resistor R_1 and the second with a matching resistor R_2 . As the structure is symmetric the even and odd mode circuit analysis gives the design procedure of the PD and hence the derivation of the exact design equations.

A. EVEN - ODD MODE ANALYSIS

As the dual-band power divider is symmetrical w.r.t. the axis, the analysis can be done using an even-odd mode. The voltage sources V_1 and V_2 are connected at the output. The impedance at port1 is divided as a combination of two parallel impedances having a value $2Z_o$. Matching resistors R_1 and R_2 are also split into two based on this symmetrical nature. Excitation corresponding to even-odd mode is then applied to the circuit.

1) Analysis at port 1 – Even mode

When even-mode excitation is applied, signals $V_1 = V_2$ with equal magnitude and phase appear at output ports. Hence the difference in voltage across the isolation resistors is absent. The circuit seems segmented with an open circuit, so it is clear that the isolation resistor is passive in even mode. So the port one impedance seems to be $2Z_o$. Admittance representation in even-odd mode operation is as in Fig. 2. The admittance at the input side (Y_{in}) of a power divider with impedance Z , resistor R_1 and electrical length θ_1 may be given by (1) based on [19].

$$Y_{in} = \left\{ \frac{R_1}{2Z^2 \sin^2 \theta_1} \right\} - \left\{ \frac{2j}{Z \tan \theta_1} \right\} \quad (1)$$

The scattering parameter at port 1 in even mode analysis is

$$S_{11e} = \frac{1 - Y_{1,in}^e 2Z_0}{1 + Y_{1,in}^e 2Z_0} \quad (2)$$

From Fig. 3 the input admittance at Port1, $Y_{1,in}^e$, with characteristic impedance Z_0 and the impedance of the two transmission line segments as $Z_{TL1} = Z_{TL2} = Z_{TL}$ gives (3) and (5):

$$Y_{1,in}^e = \left\{ \frac{1}{Z_{TL}} \right\} \left\{ \frac{Z_{TL} Y_{1,TL}^e + j \tan \theta_1}{1 + j Z_{TL} Y_{1,TL}^e \tan \theta_1} \right\} \quad (3)$$

When the condition for impedance matching of a three port reciprocal device is applied to (2), it gives the input admittance as

$$Y_{1,in}^e = \frac{1}{2Z_0} \quad (4)$$

$$Y_{1,TL}^e = \left\{ \frac{1}{Z_{TL}} \right\} \left\{ \frac{Z_{TL} + j Z_o \tan \theta_2}{Z_o + j Z_{TL} \tan \theta_2} \right\} \quad (5)$$

Comparing and rearranging (3) and (4) results in (6).

$$Z_{TL} Y_{1,TL}^e = \frac{j 2 Z_o \tan \theta_1 - Z_{TL}}{j 2 Z_{TL} \tan \theta_1 - 2 Z_o} \quad (6)$$

Similarly from (5) we get (7)

$$Z_{TL} Y_{1,TL}^e = \frac{Z_{TL} + j 2 Z_o \tan \theta_2}{Z_o + j 2 Z_{TL} \tan \theta_2} \quad (7)$$

Equating (6) and (7) to get an equation in terms of the electrical length of the two transmission line sections results in (8).

$$P \left[j Z_{TL}^2 - \left(\frac{Z_{TL} Z_o}{P} \right) (1 - Q) - j 2 Z_o \right] = 0 \quad (8)$$

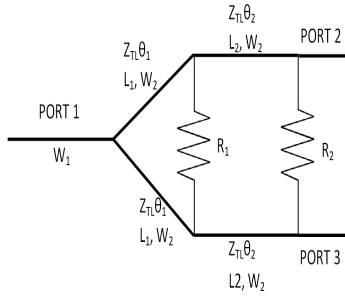


FIGURE 1. Equivalent circuit of dual band power divider

Here $P = (\tan\theta_1 + \tan\theta_2)$ and $Q = (\tan\theta_1 \tan\theta_2)$

2) Analysis at Port-2 – Even Mode

The admittance from port 2 w.r.t. Fig.2 can be given as in (8) and (9).

$$Y_{2, in}^e = \left\{ \frac{1}{Z_{TL}} \right\} \left\{ \frac{Z_{TL} Y_{2, TL}^e + j \tan\theta_2}{1 + j Z_{TL} Y_{2, TL}^e \tan\theta_2} \right\} \quad (9)$$

$$Y_{2, TL1}^e = \left\{ \frac{1}{Z_{TL}} \right\} \left\{ \frac{Z_{TL} + j 2 Z_o \tan\theta_1}{2 Z_o + j Z_{TL} \tan\theta_1} \right\} \quad (10)$$

Here $Y_{2, TL1}^e = Y_{2, TL}^e$.

Based on the procedure followed in (2),(3) and (4), from (10) we get (11).

$$P \left[j Z_{TL}^2 - \left(\frac{Z_{TL} Z_o}{P} \right) (Q - 1) - j 2 Z_o \right] = 0 \quad (11)$$

Equations (7) and(11) are added together to solve for Z_{TL} , which gives $(Z_{TL}) = \sqrt{2} Z_o$

3) Analysis at Port 2 – Odd Mode

A second order network provides matching of impedance at two frequencies f_1 and f_2 . From Fig.2 the admittance at output port, $Y_{o, TOT}$ can be found as in (12).

$$Y_{o, TOT} = \left\{ \frac{\left(\frac{1}{Y_{3o}} \right) + \left(\frac{R_2}{2} \right)}{\left(\frac{1}{Y_{3o}} \right) \left(\frac{R_2}{2} \right)} \right\} \quad (12)$$

where, $Y_{3o} = \frac{Z_{TL} + j 2 Z_o \tan\theta_2}{Z_{TL} (Z_o + j Z_{TL} \tan\theta_2)}$

The real part and the imaginary part of (12) corresponding to matching conditions at frequencies f_1 and f_2 can be rearranged into independent equations with R_1 and R_2 as unknown parameters, on solving R_1 and R_2 can be obtained as :

$$R_2 = 2\sqrt{2} Z_o \left\{ \frac{\sqrt{P \tan\theta_2 (\sqrt{2} + \sqrt{(Q-1)})}}{1 + P 2 \tan\theta_2 - Q} \right\} \quad (13)$$

$$R_1 = \left\{ \frac{2 R_2 Z_o \tan\theta_1}{(R_2 P) - 2 Z_o P} \right\} \quad (14)$$

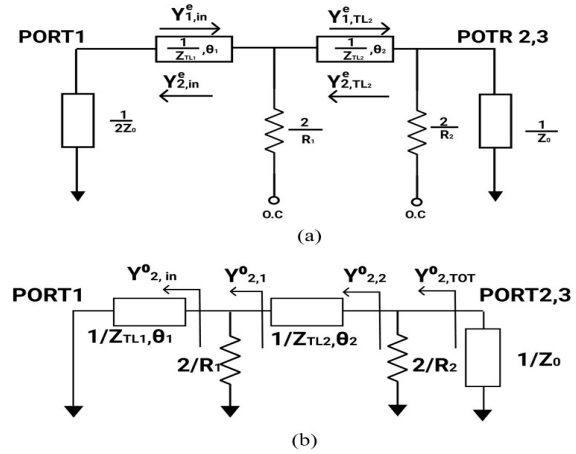


FIGURE 2. Admittance representation w.r.t. input and output ports (a). Even mode (b). Odd Mode

TABLE 1. Design parameters and dimension

f_1	f_2	$m = f_2/f_1$	W_1 (mm)	W_2 (mm)	L_1 (mm)	L_2 (mm)
2.5	7	2.8	2.5	1.414	11.63	8.597
Characteristic Impedance = 70.7Ω, R1 = 122Ω, R2=163Ω						

4) Dual band Analysis

Equations (14) and (15) have solutions at multiple electrical length values to satisfy dual-band operation. The electrical length corresponding to the desired lower and upper centre frequency of design should satisfy the relations corresponding to the electrical length of the first and second transmission line sections given by (15),

$$\theta_1 = \left[\frac{n\pi}{1+m} \right], \theta_2 = \left[\frac{mn\pi}{1+m} \right] \quad (15)$$

5) Design Procedure

Based on the design theory and analytical solutions done in the above sections, a parametric analysis is introduced in terms of electrical lengths θ_1 and θ_2 . The tuning ratio "m" and the selected centre frequencies f_1 and f_2 should satisfy the required conditions specified in (15). From the parametric analysis, the summary of the design procedure adopted for designing the DBPD model can be explained as follows:

1. Fix the centre frequency and tuning ratio and fix the impedance of the transmission line sections.
2. Determine the values of matching resistors according to (13) and (14) and the electrical length corresponding to the selected frequency as per(15).
3. Transform electrical parameters to corresponding microstrip dimensions.
4. Apply ANSYS-HFSS according to the calculated values to get the design.

III. IMPLEMENTATION, MEASUREMENT AND ANALYSIS

The dual-band power divider is designed based on the parameters indicated in Table-1.

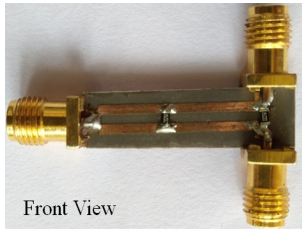


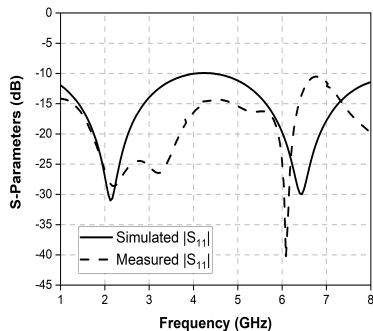
FIGURE 3. Fabricated prototype

The performance of the divider is studied by simulating the same using the software ANSYS HFSS and it is verified by fabricating a prototype. The proposed dual-band PD is realized with the substrate Rogers RT/Duroid 5880 having a height, $h = 0.8\text{mm}$, and dielectric constant of 2.2.

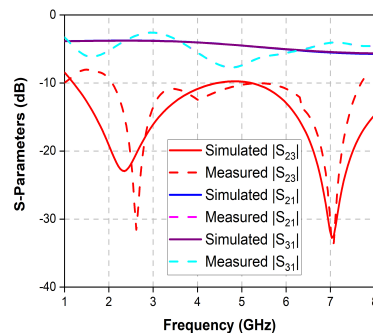
The dual-band PD is converted to microstrip at the desired frequencies of 2.5GHz and 7GHz at constant characteristic impedance but with unequal transmission line sections. As per section II’s design summary, the frequency ratio is $m = 2.8$. The corresponding electrical parameters are converted into physical quantities to get the microstrip line’s lengths and widths. The matching resistor values R_1 and R_2 are calculated. A parametric study was done to optimize the design parameters. Fig.3 corresponds to the fabricated structure of the designed dual-band power divider.

A. ANALYSIS BASED ON S PARAMETERS.

The analysis of the DB power divider is done w.r.t. scattering matrix.

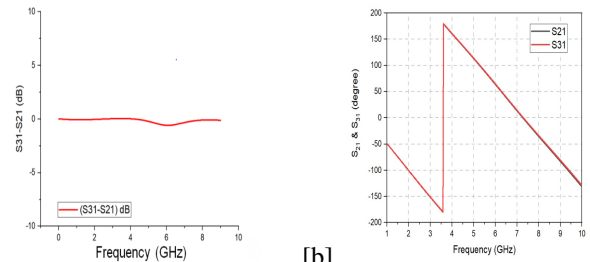


[a]



[b]

FIGURE 4. Comparison of layout simulation and measurement results of the designed circuit. (a) Input reflection (b) Isolation and Insertion loss



[a]

[b]

FIGURE 5. (a) Amplitude Difference (b) Phase response at output ports

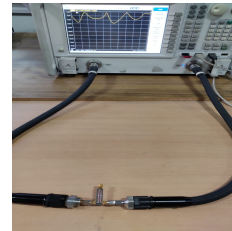


FIGURE 6. Measurement using Network Analyzer Agilent N5247A

The power divider’s performance is evaluated based on return loss, isolation between the output ports, and the insertion loss at the output ports. The performance parameters obtained based on the S matrix analysis of the dual-band power divider is shown in Fig.4 and Fig.5.

The prototype is measured with an Agilent N5247A network analyzer, and the measurement setup is shown in Fig.6.

Results indicate return loss minimum with respect to the input ports, isolation and insertion loss maximum obtained at the two desired center frequencies, f_1 and f_2 are 42/31 dB, 34/31 dB, and 3.7/4.1 dB, respectively. Results of measurement and simulation match well. The plot of phase characteristics reveals the in-phase behaviour of the power divider. One of the key issues related to practical applications is the practical operational bandwidth of the designed dual-band PD. The practical operational bandwidth is defined as the intersections of the respective bandwidth of the corresponding S-parameters. Considering this manner, the designed dual-band PD structure outperformed similar structures showing the wide practical bandwidth of nearly 2GHz at both bands. The bandwidth at the designed frequencies of the corresponding S-parameters is defined at the magnitude range of less than -15dB. The response corresponds to wideband performance at the designed frequency bands. The isolation performance states that the proposed design exhibits a good isolation level and bandwidth due to the reflection coefficient’s almost identical frequency-dependent characteristics. So this proposed DB PD features a high isolation level and wide passbands within the entire operation bands. The surface current distribution of this power divider is analyzed. It is observed as high corresponding to the two resonant frequencies at 2.5GHz and 7GHz. A significant observation from the obtained results is the -15dB bandwidth obtained at the desired frequency bands. Also, the proposed DB PD is one of the most compact-sized with a significant

TABLE 2. Table of performance comparison of the proposed DBPD with related state-of-the-art power dividers.

Ref.	Tuning ratio	Centre frequency(GHz)	Return Loss (dB)	Isolation (dB)	Isolation elements	TLs and Stubs
[7]	2	1.8/0.9	$\geq -20dB$	$\geq -40dB$	1 Resistor, 1 Capacitor, 1 Inductor	4
[9]	2.4	5.8/2.4	$\geq -20dB$	$\geq -30dB$	1 Resistor, 1 capacitor	4,3
[11]	2	2.2/1.1	$\geq -20dB$	$\geq -20dB$	1 Resistor	4,3
[17]	3.5	3.5/1	$\geq -23dB$	$\geq -25dB$	1 Resistor, 1 Inductor	5, 2
[19]	1.3	2.4/1.8	$\geq -11.9dB$	$\geq -14dB$	1 Resistor, 1 Inductor, 1 Capacitor	6
This work	2.8	7/2.5	$\geq -42/ \geq 31dB$	$\geq -34/ \geq 31$	2 Resistors	4

difference among the two centre frequencies with only four transmission line sections as per literature. The difference between the insertion loss at port two and port three shown in fig.5.(a) indicates that S_{21} is almost equal to S_{31} . This reveals that power is equally divided at the two output ports and the in-phase behaviour of the power divider is evident from fig. 5. (b). Examination of the bandwidth of the power divider w.r.t. equal power division indicates a lower operating bandwidth of 1.2GHz and an upper operating bandwidth of 1.1GHz. The constant characteristic impedance among the two sections accounts for this behaviour.

A comparison between the performance of the designed DBPD, and recent The state-of-the-art dividers are presented in Table 2. By analyzing the data, it can be observed that the proposed work provides dual-band operation with a minimum number of transmission line sections and without using reactive elements.

IV. CONCLUSION

This paper presents a transmission line structure suitable for dual-band applications based on the Wilkinson PD concept. A practical combination of the transmission line sections is done by performing rigorous analysis. This power divider provides dual-band operation centered at 2.5GHz and 7GHz frequencies. The applications of the selected frequency bands are that 2.4 GHz is the operating band of Wi-Fi, and 7GHz is used for advanced LTE and LTE WLAN and provides better uptime. The mathematical approach adopted in this design differs from that followed in other multi-section –multiband power divider designs. The analytical solution approach is based on the transfer matrix method with fixed impedance corresponding to the transmission line sections. Matching resistors between the cascaded transmission line sections contributes to better isolation and impedance matching in multiband operation. The step-by-step design procedure and the required design equations presented make prototyping much more effortless. As reactive elements are not used in the design, this DB Power divider is free from parasitic effects and provides wideband operation at centre frequencies. Also, stubs are not used in between the transmission line sections, which adds to the design’s compactness. The presented design also provides a larger tuning ratio and wide isolation band, which is highly attractive for applications related to modern wireless communication techniques.

REFERENCES

- [1] Ernest J Wilkinson. An n-way hybrid power divider. IRE Transactions on microwave theory and techniques, 8(1):116–118, 1960.
- [2] David M Pozar. Microwave engineering. John wiley & sons, 2011.
- [3] Xiaolong Wang, Zhewang Ma, and Masataka Ohira. Theory and experiment of two-section two-resistor wilkinson power divider with two arbitrary frequency bands. IEEE Transactions on Microwave Theory and Techniques, 66(3):1291–1300, 2017.
- [4] Tadashi Kawai, Yasuaki Nakashima, Yoshihiro Kokubo, and Isao Ohta. Dual-band wilkinson power dividers using a series rlc circuit. IEICE transactions on electronics, 91(11):1793–1797, 2008.
- [5] Xiaolong Wang and Iwata Sakagami. Generalized, dual-band wilkinson power divider with parallel l, c and r components. IEICE Technical Report; IEICE Tech. Rep., 113(460):53–58, 2014.
- [6] RR Sushmeetha and S Natarajamani. Compact tunable dualband bpf using edge-open srr for x-band applications. In 2018 ICACCI, pages 1624–1626. IEEE, 2018.
- [7] Yi-Hsin Pang and Zhong-He Li. Dual-band bandpass wilkinson power divider of controllable bandwidths. Electronics Letters, 52(7):537–539, 2016.
- [8] Rekha G Nair and S Natarajamani. Design of ms multi-band resonator power divider. In 2021 ICICV, pages 656–660. IEEE, 2021.
- [9] Mohammad A Maktoomi, Rahul Gupta, and Mohammad S Hashmi. A dual-band impedance transformer for frequency-dependent complex loads incorporating an l-type network. In 2015 AP Microwave Conference, volume 1, pages 1–3. IEEE, 2015.
- [10] Tso-Jung Chang, Yi-Fan Tsao, Ting-Jui Huang, and Heng-Tung Hsu. Bandwidth improvement of conventional dual-band power divider using physical port separation structure. Electronics, 9(12):2192, 2020.
- [11] Cong Wang, Bingfang Xie, Yuchen Wei, Danqing Zou, Huan Zhou, Zhongliang Zhou, Xiaofeng Gu, He Yu, Qun Wu, and Fuxing Liu. Design method of dual-band wilkinson power divider with designable length and high design freedom. AEU-International Journal of Electronics and Communications, 132:153636, 2021.
- [12] M. V. Amrutha and B. Sabarish Narayanan. Low profile patch antenna on cement substrate for indoor applications. In 2017 International Conference on Wireless

- Communications, Signal Processing and Networking (WiSPNET), pages 2508–2511, 2017.
- [13] Zihui Zhu, Zhongbao Wang, Jian Ma, Hongmei Liu, and Shaojun Fang. Dual-band balanced-to-unbalanced power divider with independent power division ratios. *IEEE Access*, 8:192659–192668, 2020.
- [14] Xiao Jia, Shao-Jun Fang, Hongmei Liu, and Zhongbao Wang. Compact dual-band wilkinson power divider terminated with frequency-dependent complex impedances. *Progress In Electromagnetics Research Letters*, 91:85–91, 01 2020.
- [15] B Naveen Reddy and V Mokaladevi. Broadband circularly polarized microstrip patch antenna with fractal defected ground structure. In *International Conference on Communication, Computing and Electronics Systems*, pages 717–724. Springer, 2020.
- [16] Fu-Xing Liu and Jong-Chul Lee. Design of new dual-band wilkinson power dividers with simple structure and wide isolation. *IEEE Transactions on Microwave Theory and Techniques*, 67(9):3628–3635, 2019.
- [17] Heba Jaradat, Nihad Dib, and Khair Al Shamaileh. Miniaturized dual-band cpw wilkinson power divider using t-network adopting series stubs with a high frequency ratio. *AEU - International Journal of Electronics and Communications*, 107:32–38, 2019.
- [18] Chatrpol Pakasiri and Sen Wang. Dual-band compact wilkinson power divider using common inductor and complex load. *IEEE Access*, 8:97189–97195, 2020.
- [19] R Gupta, Bekarys Gabdrakhimov, A. Dabarov, Galymzhan Nauryzbayev, and M.S. Hashmi. Development and thorough investigation of d.band wpd for arbitrary impedance environment. *IEEE Open Journal of the Industrial Electronics Society*, 2:401–409, 2021.